RSC Advances

This is an *Accepted Manuscript*, which has been through the Royal Society of Chemistry peer review process and has been accepted for publication.

Accepted Manuscripts are published online shortly after acceptance, before technical editing, formatting and proof reading. Using this free service, authors can make their results available to the community, in citable form, before we publish the edited article. This *Accepted Manuscript* will be replaced by the edited, formatted and paginated article as soon as this is available.

You can find more information about *Accepted Manuscripts* in the Information for Authors.

Please note that technical editing may introduce minor changes to the text and/or graphics, which may alter content. The journal's standard Terms & Conditions and the Ethical guidelines still apply. In no event shall the Royal Society of Chemistry be held responsible for any errors or omissions in this *Accepted Manuscript* or any consequences arising from the use of any information it contains.

ROYAL SOCIETY OF CHEMISTRY

www.rsc.org/advances

Please do not adjust margins

PCCP

PAPER

Electrical and Optical Polarization Responses of Composite Films Based on Aligned Carbon Nanotubes

Received 00th January 2015,
Accepted 00th January 2015

DOI: 10.1039/x0xx00000x

www.rsc.org/

Yuejiang Wen[a], Xiangdong Xu[a,b,c], Minghui Sun[a], Qiong He[a], Meng Wang[a], Yu Gu[a], Yadong Jiang[a,b], Zelin Dai[a], Zhegeng Chen[a], Tianhong Ao[a]

A simple and efficient approach for large-area preparation of horizontally-aligned carbon nanotube (CNT)–vanadium oxide (VO_x) composite films is presented. The composite films were prepared by an extended blown-bubble film approach, in which spin coating of VO_x and bubble-blowing of CNTs were combined. Results reveal that one-dimensional CNTs are well horizontally-aligned in the composite films, and the sheet resistance is significantly decreased after CNTs have been composed with VO_x. Particularly, both anisotropies of electrical and optical responses were experimentally observed in such composite films. Based on the experimental results, a model for elucidating the anisotropy of light absorption was theoretically derived. This work discloses valuable results about the novel horizontally-aligned CNT–VO_x composite films, their preparation, and peculiar electrical and optical properties.

Introduction

In the past decades, vanadium oxides (VO_x) have attracted considerable attention, owing to their distinctive electrical and optical properties. Vanadium (V) is a transition metal possessing a series of oxidation states, causing the presence of numerous VO_x, *e.g.* V_2O_5, V_6O_{13}, VO_2, V_2O_3, etc. Some VO_x with mixed oxidation states of V exhibit suitable sheet resistance and high temperature coefficient of resistance (*TCR*),[1] as well as linear electrical and optical responses, by which such VO_x are applied widely in sensors, such as gas-sensing devices[2] and especially uncooled infrared bolometric detectors[1,3]. Some other VO_x, including V_2O_5, VO_2 (A phase) and V_2O_3, undergo a reversible transition from semiconductor to metal at critical temperatures,[4] and thus they are employed as optical or electrical switches.[5] Besides, VO_2 (B phase) possesses outstanding electrochemical properties for serving as battery electrodes.[6] Therefore, vanadium oxides are important functional materials for both academic research and industrial applications.

On the other hand, one-dimensional (1D) carbon nanotubes (CNTs) with perfect period hexagons are highly attractive and widely employed since their discovery,[7] owing to their exceptional electrical, optical and mechanical properties.[8] These interesting nanomaterials hold great potential for applications as superconductors,[9] carriers of therapeutic molecules,[10] terahertz (THz) emitters or detectors,[11,12] and nano-radio atenna.[13] It has been demonstrated that composite films composed of CNTs and polymers exhibit peculiar properties,[14] so that they can be applied efficiently in light-emitting diodes,[15] photovoltaic cells,[16] memory devices,[17] and sensors.[18] Recently, we exploited CNTs to efficiently modify a THz sensitive material of 4-N,N-dimethylamino-4′-N′-methyl-stilbazolium tosylate (DAST).[19] Accordingly, it is expected that combination of VO_x and CNTs promisingly provides a possibility to further improve the physical properties of VO_x, by which new functional materials might be developed.

Although CNT–VO_x composites have been previously prepared by atomic layer deposition[20] and hydrothermal approach[21], the CNTs in those composites are distributed randomly.[20,21] It is believed that some structure-dependent phenomena could only be observed in the composites containing well-aligned CNTs. Recently, composites that are composed of VO_x and aligned CNTs were reported, and these materials exhibit excellent capacitances and are suitable for battery applications.[22,23] Unfortunately, those previous CNTs were aligned by catalyzed growth,[22,23] and thus only vertical alignment of CNTs, where the CNTs are perpendicular to the substrates, could be yielded.[22,23] Vertical alignment of CNTs in the composites strongly limits the applications of such materials in many fields, especially in electronic or optoelectronic devices, where the peculiarities in the parallel directions are required. This problem can be solved by preparing horizontally-aligned CNT–VO_x composites, in which CNTs and VO_x are parallel to the substrates. But such preparation is difficult to achieve, and consequently, to the best of our knowledge, no any literatures on horizontally-aligned CNT–VO_x composites have been reported to date. In contrast, numerous results about horizontal

[a] State Key Laboratory of Electronic Thin Films and Integrated Devices, [b] School of Optoelectronic Information, University of Electronic Science and Technology of China (UESTC), Chengdu 610054, P.R. China.
[b] Cooperative Innovation Center of Terahertz Science, University of Electronic Science and Technology of China (UESTC), Chengdu 610054, P.R. China.
[c] Corresponding author. Tel: +86-028-83208959; E-mail address: xdxu@uestc.edu.cn

Electronic Supplementary Information (ESI) available: [details of any supplementary information available should be included here]. See DOI: 10.1039/x0xx00000x

RSC Advances Accepted Manuscript

alignment of CNTs have been published and highly attractive in both fundamental and applied fields,[24-33] owing to their potential applications in high-density IC interconnects,[26] field-effect transistors,[27] polarization-dependent THz emitters or detectors.[11,12] Many methods,[24,25] including CVD growth,[26] external electric field,[28] magnetic field assembly,[29] Langmuir-Blodgett,[30] patterned chemical assembly,[31] and formation of aligned CNT fibers[32,33] have been developed for horizontally aligning CNTs. However, these previous methods are challenged in preparing horizontally-aligned CNT–VO_x composites for device applications, due to their inherent disadvantages, namely, contamination of the products by electrodes[28] or metal catalysts[26], poor efficiency,[27-33] and the trouble in preparing large-area uniform films on various substrates.[24-30]

Recently, Lieber and co-workers have developed a blown-bubble film (BBF) method for preparing horizontally-aligned 1D CNTs or nanowires.[34,35] The advantages of the BBF method include: (1) easy remove of contaminations by post-annealing; (2) capability of preparing bottom-up structured composite films; and (3) capability of producing large-area continuous films on different substrates.[34,35] Unfortunately, to the best of our knowledge, further preparation of composite films by BBF has never been reported. Herein, we extended the BBF method developed by Lieber and co-workers to successfully prepare novel horizontally-aligned CNT–VO_x composite films. Particularly, the polarization-dependent electrical and optical properties, which are critical for polarization sensing but have rarely been achieved simultaneously, of the as-prepared composite films were experimentally detected and theoretically derived in this work. Imaginably, study results about such composite films, their peculiar physical properties, and efficient preparation approaches will be considerably attractive.

Experimental Section

Briefly, the procedures for the preparation of horizontally-aligned CNT–VO_x composite films in this work involve: (1) spin coating of VO_x prepared by organic sol-gel method;[36] (2) horizontal alignment of single-walled carbon nanotubes (SWCNTs) via blown-bubble method.[34,35] In this step, the gas channel in the die is critical for blowing high-quality bubbles. We reshaped a polished stainless steel die with a frustum gas channel to smooth the incident gas,[37] where the optimal diameters of the outlet and inlet were experimentally determined to be 8.0 mm and 4.9 mm, respectively; (3) transfer of the horizontally-aligned SWCNTs to the substrates pre-coated with VO_x sol, and then annealing. The process for the preparation of horizontally-aligned CNT–VO_x composite films is illustrated in Fig. 1. Details about the modification of SWCNTs, spin coating of VO_x, bubble-blowing of SWCNTs, annealing, characterizations of the products, and other related information are described in the "Supporting Information (SI)".

Results and discussion

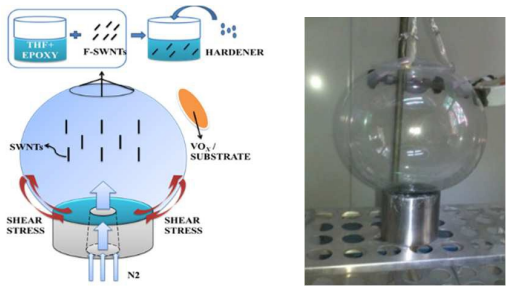

(a) (b)

Fig. 1 (a) Schematic diagram of the approach for large-area preparation of horizontally-aligned SWCNT–VO_x composite films by an extended blown-bubble film technique, and (b) photograph of a resulting blown-bubble film.

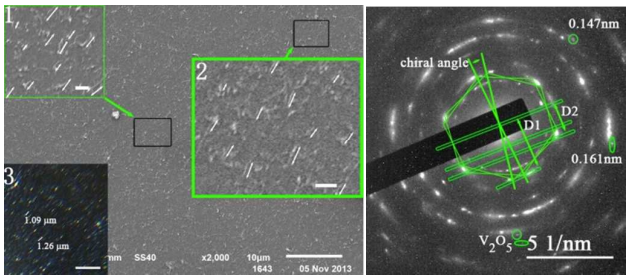

(a) (b)

Fig. 2 (a) SEM (inset 1 and 2, scale bars 1 μm) and dark-field optical microscope (inset 3, scale bar 5 μm), (b) selected-area electron diffraction pattern of a horizontally-aligned SWCNT–VOx composite film.

The surface morphologies of the as-prepared horizontally-aligned SWCNT–VO_x composite films were imaged by scanning electron microscopy (SEM), as shown in inset 1 and 2 of Fig. 2a, and dark-field optical microscope, as displayed in inset 3, respectively. Fig. 2a shows that large-area composite film has been deposited uniformly on the substrate surface by our approach. Remarkably, horizontal-alignment of 1D CNTs in the composite along the expansion direction of bubble is visible in Fig. 2a. The diameters of the SWCNTs were further estimated by Raman measurement (as described in the SI) to be 1–2 nm, in accordance with the data provided by the supplier.

The microstructures of the horizontally-aligned SWCNT–VO_x composite films were further investigated by selected-area electron diffraction (SAED) of transmission electron microscopy (TEM), and the result is shown in Fig. 2b. The discontinuous arc diffraction rings in Fig. 2b is caused by the texture effect of preferred orientation of poly-crystals,[38] implying the existence of poly-crystals in the composite films. Close inspection reveals that two hexagons overlap with a small rotated chiral angle of α that was measured to be 5.8° in Fig. 2b from the composite film. Moreover, α can be estimated with the following equation:[39]

$$\alpha = \tan\left((2 \times D2 - D1)/\left(\sqrt{3} \times D1\right)\right) \quad (1)$$

where D1=3.17 nm^{-1} and D2=1.86 nm^{-1} are the respective spacings between the reflections of principal layer lines of a carbon nanotube in the reciprocal space, as illustrated in Fig. 2b. Accordingly, α was calculated to be 5.82°, well agreeing

RSC Advances Accepted Manuscript

 This journal is © The Royal Society of Chemistry 2015

with the measurement (5.8°). Taking the α value, diameters (1–2 nm) of SWCNTs (Fig. 2a), and the parameters deduced in ref. 36 together, the chiral vector of SWCNTs was estimated to be (16,2) in the composites. Moreover, two relatively weak rings with the respective interplanar spacings of 0.147 nm and 0.161 nm, assigned to the signals of the crystal planes of V_2O_5, were simultaneously detected and marked in Fig. 2b. These demonstrate the formation of aligned CNT–VO_x composite films.

The sheet resistances (R) of the composite films prepared on glass substrates were measured at different temperatures by a high-resistance meter (HRM). Before R measurements, four electrodes with sizes of 10×10 mm^2 were deposited by thermal evaporation of cooper at four sides of the films. Although there are aligned CNTs in a BBF film without VO_x coating, its R is so high that it cannot be measured by HRM. According to previous literatures,[40,41] seldom CNTs interconnect with each other under a certain CNT concentration in a randomly orientated CNT–polymer composite**,** and thus, the conduction is dominated by the tunneling electrons in junctions between the near CNTs while ignoring the relatively low intrinsic resistivity of CNTs (10^{-6} Ω·m for CNTs with diameters of 2 nm). As revealed by SEM images (Fig. 2a), most SWCNTs are separated and do not interconnect with each other after alignment, and thereby the R of a BBF film is similarly dominated by the tunneling resistance in junctions between the neighboring CNTs. Since the distances between the near SWCNTs are enlarged after alignment, fewer electrons are able to tunnel the tubes, and thus, the R of a BBF film without VO_x is too high to be measured. But if the horizontally-aligned 1D SWCNTs have been further coated with two-dimensional (2D) VO_x film, the R of the composite film is significantly decreased so that it can be directly measured by HRM, as displayed in Fig. 3. Although residual epoxy existed in the composite, such organics is insulating and cannot enhance the conductivity. Therefore, the origin for the enhanced conductivity can only be attributed to that 2D semiconducting VO_x provides new carriers and conduct paths for the current. In this case, the horizontally-aligned but isolated 1D SWCNTs can be connected through 2D VO_x, and thus the R is drastically decreased.

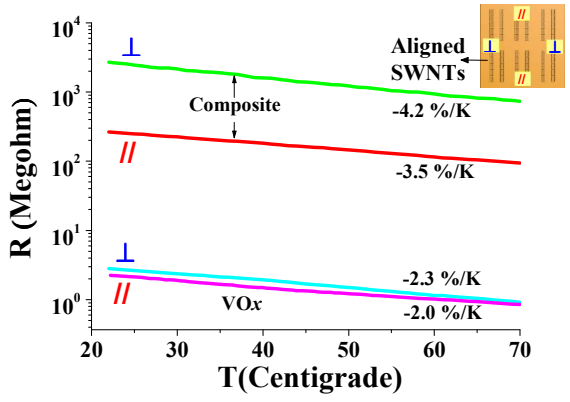

Fig. 3 Comparison of sheet resistances measured in the direction perpendicular (⊥) and parallel (//) to the axes of SWCNTs in a horizontally-aligned SWCNT–VO_x composite film and those of a pristine VO_x film measured in various directions.

Table 1 Electrical properties of a horizontally-aligned SWCNT–VO_x composite film measured in the perpendicular (⊥) and parallel (//) directions to the SWCNT axes.

	R_{RT} (MΩ)	Conductivity ($S\cdot cm^{-1}$)	*TCR* ($\%\cdot K^{-1}$)	Activation energy (eV)
Perpendicular (⊥)	2702	1.37×10^{-5}	−4.2	0.33
Parallel (//)	261	1.42×10^{-4}	−3.5	0.27

Compared with the $R_\perp$ (2702 MΩ) of a horizontally-aligned SWCNT–VO_x composite film measured at room temperature (*RT*) in the direction perpendicular (⊥) to the axes of the aligned SWCNTs, the $R_{//}$ (261 MΩ) measured in the parallel direction (//) is decreased significantly for one order of magnitude, as displayed in Fig. 3. The thicknesses of the composite films were measured to be 270±50 nm, by which the conductivities in the ⊥ and // directions were estimated to be 1.37×10^{-5} and 1.42×10^{-4} $S\cdot cm^{-1}$, respectively, close to the values of 10^{-3}–10^{-11} $S\cdot cm^{-1}$ for CNT–polymer composites.[28,29,42,43] R measurements (Fig. 3) clearly demonstrate electrical anisotropy for the horizontally-aligned SWCNT–VO_x composite films, similar to the phenomena previously observed in aligned CNT–polymer composites.[28,29,43,44] Notably, compared with those horizontally-aligned CNT–polymer composites previously prepared by electrical field[28] or magnetic field[29], the horizontally-aligned SWCNT–VO_x composite films produced in this work through BBF method exhibit larger electrical anisotropy (Fig. 3), implying well alignment of 1D CNTs in 2D VO_x (Fig. 2a) by our approach (Fig 1). According to Du[43] and Hazama[44], the conductivity of an aligned CNT–polymer composite exhibits a maximum at a specific alignment of CNTs, resulted from the competition between the number of percolating paths and the degree of meandering of the current path.[44] This conclusion also works in the aligned SWCNT–VO_x composite films. As comparison, the resistances for a pristine VO_x film measured in various directions are shown in Fig. 3. Lower R was measured, due to no epoxy existed in this film. But notably, its curve measured in the ⊥ direction matches well with that measured in the // direction, suggesting electrical isotropy for the pristine VO_x film, clearly different from electrical anisotropy observed in the horizontally-aligned SWCNT–VO_x composite film (Fig. 3).

According to Fig. 3, the *TCR* (defined as $TCR = d(\ln R)/dT = -\Delta E/(K\cdot T^2)$)[19,45] values of the horizontally-aligned SWCNT–VO_x composite films in the directions perpendicular and parallel to the SWCNT axes were calculated to be −4.2 (⊥) and −3.5 $\%\cdot K^{-1}$ (//), respectively, where ΔE, K and T are the active energy (gap between Fermi level and bottom of conducting band), Boltzmann constant, and temperature, respectively. Both *TCR* (⊥) and *TCR* (//) values in this work are obviously different from the positive *TCR* values measured in the organics,[19] and particularly, they are also much larger than those of randomly dispersed SWCNTs (~−1 $\%\cdot K^{-1}$)[9] or VO_x films (−2.0 to −2.3 $\%\cdot K^{-1}$, as shown in Fig. 3). Large *TCR* for the composite film can be attributed to the synergistic effects of 1D SWCNTs and 2D VO_x. The ΔE were calculated and summarized in Table 1. For the composite film, ΔE (⊥) = 0.33 eV is larger than ΔE (//) = 0.27 eV (Table 1). This

RSC Advances Accepted Manuscript

difference can be explained by the peculiarity of 1D SWCNTs. It is known that the states of the π electrons of SWCNTs are close to Fermi level,[46,47] and they play an important role for the electrical properties. The π electrons are easily percolated from the sidewalls of SWCNTs, which is assisted by hot phonons[48] and further promoted by 2D VO_x matrix as in this work. If the temperature rises, the number of hot phonons will increase, and thus, the number of phonon-assisted electrons percolated from the sidewalls will also increase. Since π bonds orientate perpendicular to the surface of SWCNT (perpendicular to the axis of SWCNT),[47] more phonon-assisted electrons are percolated in the direction perpendicular to the axes of SWCNTs than that in the // direction, thus leading to larger *TCR* measured in the ⊥ direction. It is clear that both *R* and *TCR* results (Fig. 3) reveal electrical anisotropy for the resulting horizontally-aligned SWCNT–VO_x composite films, due to well horizontal alignment of 1D SWCNTs in 2D VO_x.

Finally, the optical properties of the horizontally-aligned SWCNT–VO_x composite films were investigated. The UV-Vis absorption spectra were measured at *RT* by vertically incident polarized light (1.1–4.0 eV) with various polarized angles (θ) of 0°, 15° and 30°, which results are displayed in Fig. 4. In our work, θ is defined as the angle between the electrical field of incident light and the axes of SWCNTs. Interestingly, the spectra obtained at various θ are different (Fig. 4). Since the temperature remained unchanged during optical measurements, the thermal effects on the optical properties can be ignored.[49] Thus, Fig. 4 suggests that the horizontally-aligned SWCNT–VO_x composite film also exhibits anisotropic response to polarized light, similar to the electrical response (Fig. 3).

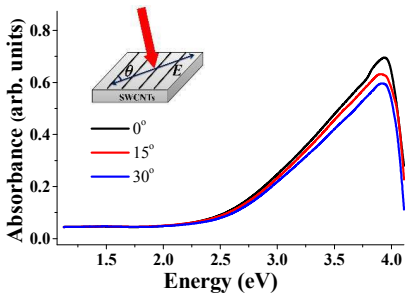

Fig. 4 UV-Vis spectra of a horizontally-aligned SWCNT–VO_x composite film measured at different polarization angles to the axes of SWCNTs.

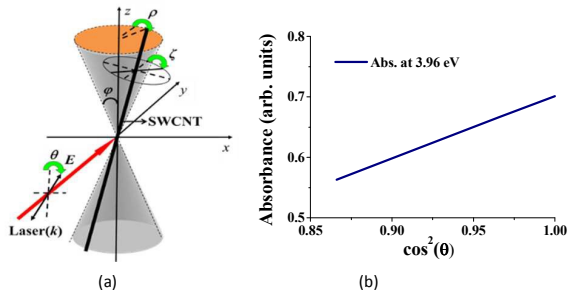

(a) (b)

Fig. 5 (a) The Cartesian-coordinate model of optical absorption, (b) the plot of absorbance at 3.96 eV vs $\cos^2(\theta)$, where θ is the polarization angle to the axes of SWCNTs.

The optical characteristics of the CNT–based composite films are originated from their unusual structures.[50] It was revealed that SWCNTs with cylindrical and period nanoscale-hexagons structures exhibit Van Hove singularities,[51] which present as cleavage of valence and conduction band and contribute to the selected wavelengths for the first (E_{11}) and second (E_{22}). transitions, and etc.[52] For the SWCNTs with a chiral vector of (16,2), as utilized in this work, E_{11} and E_{22} were estimated to be located at 0.79 and 1.26 eV detectable by spectrofluorimetric.[52] However, E_{11} and E_{22} were not observed in our UV-Vis measurements (Fig. 4). This might be resulted from the negative effects of relatively strong absorption of VO_x and the residual epoxy resin, compared with that of SWCNTs, and thus, it is hard to observe the E_{11} and E_{22} peaks. Consequently, only anisotropy of absorption at 3.96 eV is observed in the composite films (Fig. 4). Where does the peak at 3.96 eV come from? It was reported that surface π-electrons excitations of SWCNTs lead to presence of a peak at ~4.0 eV in electron energy loss spectra (EELS).[53] Similarly, electron density-functional calculations of Yang[54] and Cho[55] revealed that the imaginary part of dielectric function has a maximum at ~3.96 eV if a light is polarized parallel with the SWCNT axes. Thus, we believe that the light absorption at 3.96 eV (Fig. 4) is originated from the surface π-electrons of graphitic planes of SWCNTs in the composite. It is worth noting that the absorbance at 3.96 eV increases with θ (Fig. 4), as predicted by Yang[54] and Cho[55] through simulations on CNTs. However, for a pristine VO_x film or a pristine epoxy film, neither the peak at ~3.96 eV nor absorption varied with the polarized angle was measured. These further confirm anisotropic optical response for the horizontally-aligned SWCNT–VO_x composite films, resulted from the well horizontally-aligned SWCNTs.[46] To the best of our knowledge, this is the first presentation about such horizontally-aligned SWCNT–VO_x composite films, their preparation, electrical properties of *R*, alterations of *R* with temperature, *TCR*, and particularly, their unique electrical and optical anisotropies, all of which are highly valuable and have never been reported previously. Such composite films hold great potential for applications in polarization detection.

Based on the results in Fig. 4, the anisotropy of optical absorption can be theoretically deduced. A Cartesian coordinate is set as follow (Fig. 5a): *x* axis and *y*-*z* plane are parallel with the normal of substrate and substrate plane, respectively. And $\boldsymbol{k}$ is a propagation vector of an incident light along with *y*-axis. The $\boldsymbol{\varphi}$ ($0 \le \boldsymbol{\varphi} \le \pi/2$) is a deviation angle of SWCNT axis *C*-axis from *z*-axis, and $\boldsymbol{\rho}$ ($0 \le \boldsymbol{\rho} \le 2\pi$) is a rotational angle from *y*-*z* plane to a plane constructed by the *C*-axis and *z*-axis. A unit of aligned SWCNT–VO_x is assumed to have a collinear dipole $\boldsymbol{\mu}_{//}$ parallel with *C*-axis, and a non-collinear dipole $\boldsymbol{\mu}_{\perp}$ perpendicular to *C*-axis. $\boldsymbol{\zeta}$ ($0 \le \boldsymbol{\zeta} \le 2\pi$) is a circumferential angle between a dipole and *y*-axis, then $\boldsymbol{\mu}_{//}$ and $\boldsymbol{\mu}_{\perp}$ are expressed as:[56]

$$\boldsymbol{\mu}_{//} = \mu_{//}(\sin\varphi\cos\rho \quad \sin\varphi\sin\rho \quad \cos\varphi) \qquad (2)$$

RSC Advances Accepted Manuscript

This journal is © The Royal Society of Chemistry 2015

$$\boldsymbol{\mu}_{\perp} = \mu_{\perp}(\zeta = 0)\cos\zeta + \mu_{\perp}(\zeta = \pi/2)\sin\zeta \quad (3)$$

Here,

$$\boldsymbol{\mu}_{\perp}(\zeta = 0) = \mu_{\perp}(\sin\rho \quad \cos\rho \quad 0) \quad (4)$$

$$\boldsymbol{\mu}_{\perp}(\zeta = \pi/2) = \mu_{\perp}(\cos\varphi\cos\rho \quad \cos\varphi\sin\rho \quad \sin\varphi) \quad (5)$$

Assume a polarized light polarized is propagated with a polarization angle θ ($0 \le \theta \le \pi/2$) from *y*-*z* plane (p-plane), the electron vector is written as $\boldsymbol{E} = E(\sin\theta \quad 0 \quad \cos\theta)^{\mathrm{T}}$. Since the dipole transition probability is related to $|\boldsymbol{\mu}\cdot\boldsymbol{E}|^2$,[56] where $\boldsymbol{\mu}$ donates the dipole moment, $\boldsymbol{E}$ is the electric field of light, the absorbance of the polarized light by collinear dipoles can be expressed as:

$$\Delta_{//}(\theta) = |\boldsymbol{\mu}_{//}\cdot\boldsymbol{E}|^2 = \int_0^{2\pi}\Lambda_{//}(\theta \quad \varphi)\,d\varphi = \frac{1}{2}\mu_{//}^2\cdot E^2\left[\frac{\pi}{8} + \left(\frac{\pi^2}{2} - \frac{\pi}{8}\right)\cdot\cos^2\theta\right] \quad (6)$$

Where

$$\Delta_{//}(\ \theta \quad \rho \quad \varphi) = \mu_{//}^2\cdot E^2(\sin\varphi\cos\rho\sin\theta + \cos\varphi\cos\theta)^2 \quad (7)$$

$$\Delta_{//}(\theta \quad \varphi) = \int_0^{2\pi}\Lambda_{//}(\ \theta \quad \rho \quad \varphi)\,d\rho \quad (8)$$

In fact, the deviation angle is assumed to have a distribution described by a probability function *f(φ)* after the alignment of SWCNTs. Consequently, the experimentally observed absorbance will be:

$$\Delta_{//}^{'}(\theta) = \int_0^{\pi/2}\Lambda_{//}(\theta \quad \varphi)f(\varphi)\,d\varphi \Big/ \int_0^{2\pi}\mathrm{f}(\varphi)\,d\varphi = a + b\cdot\cos^2\theta \quad (9)$$

For a given as-prepared film, *a* and *b* constants are:

$$a = \frac{1}{2}\mu_{//}^2\cdot E^2(1 - \langle\cos^2\varphi\rangle) \quad (10)$$

$$b = \frac{1}{2}\mu_{//}^2\cdot E^2(-1 + (1 + 4\pi)\langle\cos^2\varphi\rangle) \quad (11)$$

Similarly,

$$\Delta_{\perp}^{'}(\theta) = c + d\cdot\cos^2\theta \quad (12)$$

Here,

$$c = \frac{1}{2}\mu_{\perp}^2\cdot E^2(\frac{1}{2} + \frac{1}{2}\langle\cos^2\varphi\rangle) \quad (13)$$

$$d = \frac{1}{2}\mu_{\perp}^2\cdot E^2(-\frac{1}{2} + 2\pi - \left(\frac{1}{2} + 2\pi\right)\langle\cos^2\varphi\rangle) \quad (14)$$

Therefore,

$$\Delta(\theta) = \Delta_{//}^{'}(\theta) + \Delta_{\perp}^{'}(\theta) = \mathrm{a} + \mathrm{c} + (\mathrm{b} + \mathrm{d})\cdot\cos^2\theta \quad (15)$$

Above theoretical deduction reveals that if 1D SWCNTs are well horizontally-aligned in a composite, a linear relationship between the absorbance $\Delta(\theta)$ and $\cos^2\theta$ would be experimentally observed. Fig. 5b shows a plot of absorbance at 3.96 eV of the composite film in Fig. 4 *versus* $\cos^2\theta$. Remarkably, a linear relationship between the absorbance and $\cos^2\theta$ is acquired in Fig. 5b. This gives evidence for that the anisotropy of optical response (Fig. 4) is essentially induced by the well horizontally-aligned SWCNTs in the composite film, as suggested by the dipole transition model.

Conclusions

In summary, by combining the conventional spin coating technique, we extended the blown-bubble film method to successfully prepare novel polarization-dependent horizontally-aligned SWCNT–VO_x composite films. The structures and physical properties of the as-prepared composite films were systematically investigated. Results reveal that 1D SWCNTs are well horizontally-aligned in the composite films, thus leading to that both the electrical properties of sheet resistances and *TCR* of the composite films measured in the direction parallel to the axes of SWCNTs are significantly smaller than those measured in the perpendicular direction. Moreover, optical absorption of the composite films varies with the incident angle, and anisotropy of light absorption at 3.96 eV was experimentally observed and theoretically verified. Thus, we conclude that such composite films exhibit both electrical and optical anisotropies. These novel horizontally-aligned SWCNT–VO_x composite films with peculiar nanostructure-controlled electrical and optical properties hold great potential for future academic research and industrial applications, especially for polarization-dependent optoelectronic detectors. Particularly, the strategy described in this work can be easily extended to prepare other horizontally-aligned nanomaterial–based composites.

Acknowledgements

Financial support of this work by the National Natural Science Foundation of China (NSFC 61071032, 61377063, 61235006, 61421002) is acknowledged. And the authors would like to thank Dr. Xiaotong Zheng from South West Jiaotong University for TEM characterization.

References

1 W. A. Radford, D. F. Murphy, M. Ray, S. H. Propst, A. Kennedy, J. K. Kojiro, J. Woolaway and K. Soch, *Proc. SPIE,* 1996, **2746**, 82-92.
2 M. G. Willinger, G. Neri, E. Rauwel, A. Bonavita, G. Micali and N. Pinna, *Nano Lett.*, 2008, **8**, 4201–4204.
3 P. W. Kruse, W. A. Bellingham, *SPIE press*, 2001.
4 F. J. Morin, *Phys. Rev. Lett.,* 1959,**3**, 34-36.
5 D. P. Partlow, S. R. Gurkovich, K. C. Radford and L. J. Denes, *J. Appl. Phys.,* 1991, **70**, 443-452.
6 E. Baudrin, G. Sudant, D. Larcher, B. Dunn and J. M. Tarascon, *Chem. Mater.,* 2006, **18**, 4369-4374.
7 S. Iijima, *Nature,* 1991, **354**, 56-58.
8 R. H. Baughman, A. A. Zakhidov and W. A. de Heer, *Science,* 2002, **297**, 787-792.
9 M. E. Itkis, F. Borondics, A. Yu and R. C. Haddon, *Science,* 2006, **312**, 413-416.
10 K. Kostarelos, L. Lacerda, G. Pastorin, W. Wu, S. Wieckowski, J. Luangsivilay, S Godefroy, D Pantarotto, J. P. Briand, S Muller, M Prato and A Bianco. *Nat. Nanotechnol.,* 2007, **2**, 108-113.
11 L. Ren, Q. Zhang, C. L. Pint, C. L. Pint, A. K. Wójcik, M. Bunney, T. Arikawa, I. Kawayama, M. Tonouchi, R. H. Hauge, A. A. Belyanin and J. Kono, *Phys. Rev. B,* 2013, **87**, 161401.
12 B. Heshmat, H. Pahlevaninezhad, M. C. Beard, C. Papadopoulos and T. E. Darcie, *Opt. express,* 2011, **19**, 15077-15089.

RSC Advances Accepted Manuscript

13 K. Jensen, J. Weldon, H. Garcia, H. Garcia and A. Zettl, *Nano lett.,* 2007, **7**, 3508-3511.
14 L. Li, Z. Yang, H. Gao, H. Zhang, J. Ren and X. Sun, *Adv. Mater.,* 2011, **23**, 3730-3735.
15 R. C. Smith, J. D. Carey , R. J. Murphy, W. J. Blau, J. N. Coleman and S. R. P. Silva, *Appl. Phys. Lett.,* 2005, **87**, 263105.
16 S. Berson, R. de Bettignies, S. Bailly, S. Guillerez and B. Jousselme, *Adv. Funct. Mater.,* 2007, **17**, 3363-3370.
17 J. Li, Q. Ye, A. Cassell, H. T. Ng, R. Stevens, J. Han and M. Meyyappan, *Appl. Phys. Lett.,* 2003, **82**, 2491-2493.
18 H. Peng, X. Sun, F. Cai, F. Cai, X. Chen, Y. Zhu, G. Liao, D. Chen, Q. Li, Y. Lu, Y. Zhu and Q. Jia, *Nat. Nanotechnol.,* 2009, **4**, 738-741.
19 X. Xu, L. Huang, K. Fan, K. Fan, Y. Jiang, Z. Sun, Q. He, T. Ao, R. Huang, Y. Wen and C. Ma, *J. Mater. Chem. C,* 2014, **2**, 2394-2403.
20 M. G. Willinger, G. Neri, E. Rauwel, A. Bonavita, G. Micali and N. Pinna, *Nano lett.,* 2008, **8**, 4201-4204.
21 L. Liang, H. Liu and W. Yang, *Nanoscale,* 2013, **5**, 1026-1033.
22 W. Lu, A. Goering, L. Qu and L. Dai, *Phys. Chem. Chem. Phys.,* 2012, **14**, 12099-12104.
23 P. H. Jampani, K. Kadakia, D. H. Hong, R. Epur, J. A. Poston, A. Manivannan and P. N. Kumta, *J. Electrochem. Soc.,* 2013, **160**, A1118-A1127.
24 Y. Ma, B. Wang, Y. Wu, Y. Huang and Y. Chen, *Carbon*, 2011, **49**, 4098-4110.
25 A. Saha, C. Jiang and A. A. Martí, *Carbon*, 2014, **79**, 1-18.
26 M. Hofmann, D. Nezich and J. Kong, *Nano lett.,* 2008, **8**, 4122-4127.
27 M. C. LeMieux, M. Roberts, S. Barman, Y. W. Jin, J. M. Kim and Z. Bao, *Science,* 2008, **321**, 101-104.
28 Y. F. Zhu, C. Ma, W. Zhang, R. P. Zhang, N. Koratkar and J. Liang, *J. Appl. Phys.,* 2009, **105**, 054319.
29 T. Kimura, H. Ago, M. Tobita, S. Ohshima, M. Kyotani and M. Yumura, *Adv. Mater.,* 2002, **14**, 1380-1383.
30 J. H. Lee, W. S. Kang, G. H. Nam, S. W. Choi and J. H. Kim, *J. Nanosci. Nanotechnol*., 2009, **9**, 7080-7084.
31 M. Lee, J. Im, B. Y. Lee, S. Myung, J. Kang, L. Huang, Y. K. Kwon, S. Hong, *Nat. Nanotechnol.,* 2006, **1**, 66-71.
32 C. Jiang, A. Saha, C. Xiang, C. C. Young, J. M. Tour, M. Pasquali and A. A. Martí, *ACS Nano*, 2013, **7**, 4503-4510.
33 C. Jiang, A. Saha, C. C. Young, D. P. Hashim, C. E. Ramirez, P. M. Ajayan, M. Pasquali and A. A. Martí, *ACS Nano*, 2014, **8**, 9107-9112.
34 G. Yu, A. Cao and C. M. Lieber. *Nat. Nanotechnol.*, 2007, **2**, 372-377.
35 G. Yu, X. Li C. M. Lieber and A. Cao, *J. Mater. Chem.,* 2008, **18**, 728−734.
36 X. Xu, S. Yang, Y. Jiang, D. Zhou and W. Dan, *Chinese Patent*, CN101900607 B, 2012.
37 K. Cantor, Hanser Gardner Pub. 2006.
38 D. B. Williams and C. B. Carter, Springer US, 2009, 3-22.
39 L. C. Qin, *Rep. Prog. Phys.,* 2006, **69**, 2761.
40 Y. Yu, G. Song and L. Sun, *J. Appl. Phys.,* 2010, **108**, 084319.
41 C. Li, E. T. Thostenson and T. W. Chou, *Appl. Phys. Lett.,* 2007, **91**, 223114.
42 T. McNally, P. Pötschke, P. Halley, M. Murphy, D. Martinc, S. E. J. Bell, G.P. Brennan, D. Bein, P. Lemoine and J. P. Quinn, *Polymer,* 2005, **46**, 8222-8232.
43 F. Du, J. E. Fischer and K. I. Winey, *Phys. Rev. B,* 2005, **72**, 121404.
44 Y. Hazama, N. Ainoya, J. Nakamura and A. Natori, *Phys. Rev. B,* 2010, **82**, 045204.
45 X. Xu, Z. Sun, K. Fan, Y. Jiang, R. Huang, Y. Wen, Q. He and T. Ao, *Sci. Rep.,* 2015, **5**, 12269.
46 M. Machón, S. Reich, C. Thomsen, D. Sánchez-Portal and Ordejón, *Phys. Rev. B,* 2002, **66**, 155410.
47 A. Swan, Boston University.
48 A. Nojeh, ISRN *Nanomaterials,* 2014, 2014.
49 H. Xu, S. Alur, Y, Wang, et al. *J. Electron. Mater.*, 2010, 39, 2237-2242.
50 S. Reich, C. Thomsen and J. Maultzsch, John Wiley & Sons, 2008.
51 R. B. Weisman and S. Subramoney, *Electrochem. Soc. Interface,* 2006, **15**, 42.
52 R. B. Weisman and S. M. Bachilo, *Nano Lett.,* 2003, **3**, 1235-1238.
53 B. W. Reed and M. Sarikaya, *Phys. Rev. B,* 2001, **64**, 195404.
54 X. Yang, G. Wu, J. Zhou and J. Dong, *Phys. Rev. B,* 2006, **73**, 235403.
55 T. H. Cho, W. S. Su, T. C. Leung, W. Ren and C. T. Chan, *Phys. Rev. B,* 2009, **79**, 235123.
56 Y. Murakami, E. Einarsson, T. Edamura and S. Maruyama, *Carbon,* 2005, **43**, 2664-2676.

RSC Advances Accepted Manuscript

 This journal is © The Royal Society of Chemistry 2015